IN-SITU CALIBRATION AND TRAJECTORY ENHANCEMENT OF UAV AND BACKPACK LIDAR SYSTEMS FOR HIGH-RESOLUTION FOREST INVENTORY

T. Zhou [1], R. Manish [1], S. Fei [2], and A. Habib [1] *

[1] Lyles School of Civil Engineering, Purdue University, West Lafayette, IN 47907, USA - (zhou732, rmanish, ahabib)@purdue.edu
[2] Forestry and Natural Resources, Purdue University, West Lafayette, IN 47907, USA - sfei@purdue.edu

KEY WORDS: LiDAR, feature extraction/matching, Backpack MMS, UAV MMS, system calibration, GNSS/INS trajectory enhancement, forest inventory

ABSTRACT:

Using remote sensing modalities for forest inventory has gained increasing attention in the last few decades. However, tools for deriving accurate tree-level metrics are limited. This paper investigates the feasibility of using LiDAR units onboard uncrewed aerial vehicle (UAV) and Backpack mobile mapping systems (MMS) equipped with an integrated Global Navigation Satellite System/Inertial Navigation System (GNSS/INS) to provide high quality point clouds for accurate, high-resolution forest inventory. To improve the quality of acquired point clouds, a system-driven strategy for mounting parameters refinement and trajectory enhancement using terrain patches and tree trunks is proposed. To evaluate the performance of the proposed strategy, two UAV and one Backpack datasets covering a forest plantation are used in this study. Through sequential system calibration and trajectory enhancement, the spatial accuracy of the UAV point clouds improves from 20 cm to 5 cm. For the Backpack dataset, when the initial trajectory is of reasonable accuracy, conducting trajectory enhancement significantly improves the alignment of the point cloud from 30 cm to 3cm. For a lower-quality trajectory, using the UAV data as a reference, the misalignment is reduced from 1 m to 3 cm.

1. INTRODUCTION

Traditional method for forest inventory is labour intensive, expensive, and time-consuming. Advances in algorithmic technology and remote sensing capabilities using LiDAR and photogrammetry based on aerial and terrestrial platforms have recently been explored as alternatives for automated tree-level inventory at various scales. These sensors/platforms have trade-offs in terms of cost, spatial coverage, spatial resolution, field survey efficiency, and level of detail of the acquired information (Beland et al., 2019; Kelly and Tommaso, 2015).

Manned airborne platforms, which have a large spatial coverage, have been explored in forestry research for estimating inventory attributes such as tree/canopy height, stem map/volume, and basal area, using imagery and LiDAR data (White et al., 2016). On the other hand, uncrewed aerial vehicles (UAVs) have the advantage of low cost, ease of deployment, rapid data acquisition, and ability to deliver fine resolution product at a higher frequency of field surveys. Several studies have used UAV imagery and LiDAR data to derive forest biometrics, including tree/canopy height, diameter at breast height (DBH), and above-ground biomass (Goodbody et al., 2019; Khosravipour et al., 2014). Another popular mean for determining various inventory attributes is by using terrestrial mapping platforms, including terrestrial laser scanner (TLS) and mobile ground LiDAR (UAV or backpack-mounted systems). These systems have the advantage of capturing below-canopy information (Barbeito et al., 2017; Su et al., 2020). Both the TLS and mobile ground LiDAR have been used to generate stem map, estimate DBH, and segment tree crown. Nevertheless, these platforms have their own challenges. TLS data acquisitions are complex and processing large datasets can be time-consuming. Most of the mobile ground platforms are equipped with GNSS/INS sensors crucial for deriving accurately georeferenced mapping products from the onboard sensors. Their main challenge is the limited GNSS signal reception under tree canopy that impacts the quality of resulting mapping products.

Several studies have proposed methods to tackle mapping in GNSS challenging environments. One of those popular approaches is by enhancing platform trajectory using well-defined geometric features identified and extracted from successive LiDAR frames for odometry and trajectory optimization (Chiella et al., 2019; Kukko et al., 2017; Qian et al., 2017). Results from these approaches have shown a significant improvement in the accuracy of estimated metrics, e.g., DBH, tree height, and trunk locations. However, research on improving the quality of mapping products from mobile terrestrial remote sensing systems still lacks in terms of (a) partially refining positional or attitude information, (b) inability to adjust LiDAR mounting parameters, (c) requiring extensive pre-processing for deriving suitable features for trajectory enhancement, (d) not taking full advantage of onboard IMUs, (e) limiting the range of acquired data to few meters, (f) not providing georeferenced products that could aid tracking of forest growth from temporal data acquisitions, and (g) being quite complex for scalable implementation.

In response to the above-stated limitations of the state-of-the-art techniques, this study proposes a system-driven framework capable of conducting system calibration and trajectory enhancement for LiDAR units mounted on mobile LiDAR systems (UAV or Backpack) to generate accurate point clouds for forest inventory. By minimizing discrepancies among features captured from different timestamps/tracks and different systems while considering both absolute and relative positional/rotational information provided by the GNSS/INS-based trajectory, system calibration parameters and trajectory information are refined through a non-linear least squares adjustment (LSA) process. The remainder of this paper is structured as follows: Section 2 introduces the UAV/Backpack

* Corresponding author

MMS followed by a description of the datasets used in this study; Section 3 proposes a system-driven strategy for system calibration and trajectory enhancement utilizing terrain patches and tree trunks extracted from LiDAR point clouds; Section 4 presents preliminary results based on the proposed approach using UAV and Backpack datasets; Finally, Section 5 summarizes the findings of the research presented in this paper along with recommendations for future work.

2. ACQUISITION SYSTEMS AND DATASETS DESCRIPTION

Three datasets were acquired for this study over a forest plantation using two UAV and one Backpack MMS. These systems were developed by the Digital Photogrammetry Research Group at Purdue University. The details of the mapping systems and acquired datasets are described below.

2.1 UAV and Backpack MMS

Two UAV systems were used in this study, denoted as *UAV-1* and *UAV-2*. The *UAV-1* system (as shown in Figure 1a) consists of a Velodyne VLP-32C LiDAR and a Sony α7R III camera. The payload of the *UAV-2* system is the same as *UAV-1* except for its camera, which is a Sony α7R camera. The rotation axes of the LiDAR units on both UAV systems are set to be approximately parallel to the flying direction. For both systems, the LiDAR data is directly georeferenced through an Applanix APX15 v3 GNSS/INS unit. The unit, with an IMU data rate of 200 Hz, provides a post-processing accuracy of 2–5 cm for position, 0.025° for roll/pitch angles, and 0.080° for heading angle under open sky conditions. The Backpack MMS (as shown in Figure 1b) comprises a Velodyne VLP-16 Hi-Res LiDAR and a Sony α7R II camera. A Novatel SPAN-CPT GNSS/INS is used for direct georeferencing of the LiDAR data. For this unit, the IMU data rate is 100 Hz, and it provides a post-processing accuracy of 1–2 cm for position, 0.008° for roll/pitch angles, and 0.026° for heading angle under open sky conditions.

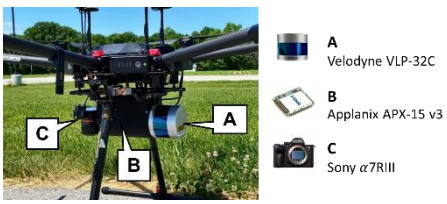

(a)

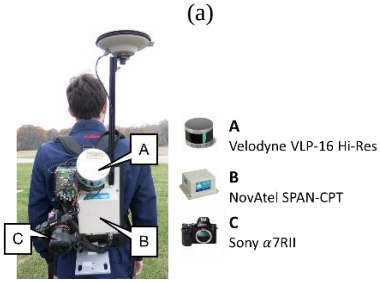

(b)

Figure 1. The mobile mapping systems and onboard sensors used in this study: (a) *UAV-1* system and (b) Backpack system.

The UAV and Backpack MMS have undergone a rigorous system calibration to estimate the mounting parameters – lever arm and boresight angles – relating onboard LiDAR sensors to the GNSS/INS unit (Ravi et al., 2018a). The expected accuracy of the point cloud following the system calibration was estimated based on the individual sensor specifications using a LiDAR Error Propagation Calculator (Habib et al., 2006); for the UAV MMS flying at a height of 50 m, the calculator suggests horizontal and vertical accuracy values in the 5–6 cm range at the nadir position. At the edge of the swath, the horizontal accuracy would be about 8–9 cm and the vertical accuracy would still be in the 5–6 cm range. For the Backpack system, the calculator suggests an accuracy of 3 cm at a range of 50 m.

2.2 Study Site and Dataset Description

The study site used for this research is a forest plantation (Plot 115 shown in Figure 2) located at Martell Forest, a research forest owned and managed by Purdue University, in West Lafayette, IN, USA. The plot follows a grid pattern consisting of 22 rows with 50 trees in each row. The total number of trees varied over time because of a tree thinning activity. In 2021, there were reportedly 1080 trees whereas by March 2022, 410 trees were cut down.

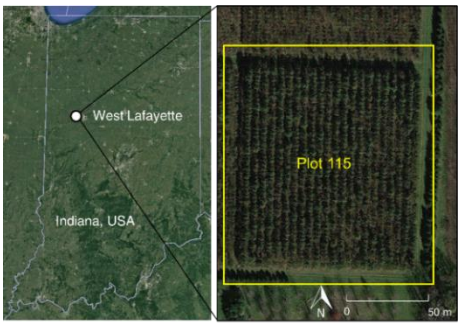

Figure 2. Study site at Martell Forest (Plot 115) consisting of 22 rows with 50 trees per row (aerial photo adapted from a Google Earth Image)

A total of three LiDAR datasets were acquired at the study site on different dates, as listed in Table 1. Two UAV datasets, one from each platform, were collected under leaf-off conditions to capture the highest possible under-canopy details. On the other hand, one Backpack dataset was acquired under leaf-on condition, representing GNSS/INS challenged environment. It is important to mention that the *UAV-2022* dataset had fewer trees due to tree-thinning activities prior to this data collection. Figure 3 shows the top view of the two UAV flight trajectories. Figure 4 shows a sample tree from the two UAV datasets where LiDAR points with large range measurements come from flight lines with large planimetric distances to this tree. The difference in noise level between *UAV-2021* and *UAV-2022* point clouds, particularly in the X direction (along-flight direction), is much higher compared to that in the Y direction (across-flight direction). This indicates that the mounting parameters of the *UAV-2* system are out-of-date (assuming the GNSS/INS trajectory is accurate).

Dataset	Platform	Date	Leaf condition	Flying height (m)	Flying speed (m/s)	Lateral distance (m)	Number of tracks
UAV-2021	*UAV-1*	March 13, 2021	Leaf-off	40	3.5	11	12
UAV-2022	*UAV-2*	March 3, 2022	Leaf-off	40	3.5	13	10
BP-2021	Backpack	August 5, 2021	Leaf-on	-	-	-	22

Table 1. Field datasets used in this study.

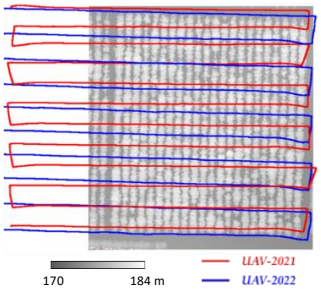

Figure 3. Top view of the flight trajectory for the two UAV datasets overlaid on the point cloud (coloured by height) captured in the *UAV-2021* dataset.

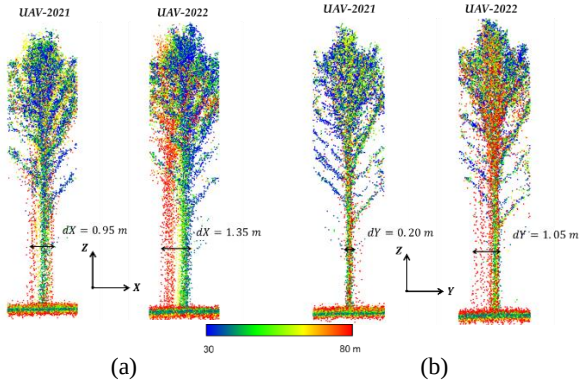

(a) (b)

Figure 4. A sample tree (colored by LiDAR range) in the *UAV-2021* and *UAV-2022* datasets viewed from (a) X-Z and (b) Y-Z planes.

To evaluate the performance of the proposed approach on the Backpack dataset, two trajectories with different quality levels were derived from GNSS/INS post-processing. The first one, denoted as original trajectory, was generated using all available GNSS satellites where the trajectory is assumed to have reasonable accuracy. From the trajectory quality report, the largest expected standard deviation was 0.4 m for the Z coordinate and 0.04° for the heading angle. To simulate a further degraded trajectory quality from GNSS signal outages, a second trajectory was generated by removing 5 satellite observations between the 4th and 19th tracks. In this case, the largest standard deviation was reported to be 1.2 m for the Z coordinate and 0.05° for the heading angle. Figure 5 shows the two Backpack trajectories generated based on the above description. One can clearly see the difference between the two versions.

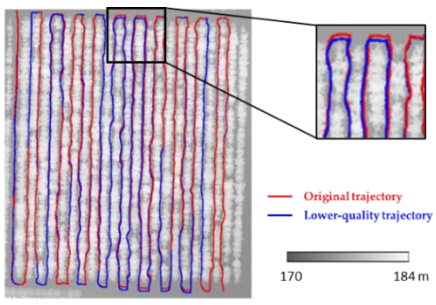

Figure 5. Original and lower-quality Backpack trajectories (for the *BP-2021* dataset) overlaid on the point cloud (colored by height) captured in the *UAV-2021* dataset.

Figure 6 illustrates the impact of GNSS signal outages on the quality of Backpack point cloud. A small region of interest (ROI) in the middle portion of row 13 (from the west) within the forest plantation is reconstructed using the original Backpack trajectory. A misalignment of about 1.7 m in horizontal direction and 1.2 m in vertical direction is observed in the point cloud. A significantly worse misalignment is expected from the lower-quality trajectory. It is worth mentioning that, for the Backpack system, the impact of potentially erroneous mounting parameters on the resulting 3D coordinates of LiDAR points is negligible compared to that by inaccurate trajectory given the short sensor-to-object distance. Therefore, the objective of the conducted experiments for the *BP-2021* dataset is trajectory enhancement while the mounting parameters are assumed errorless.

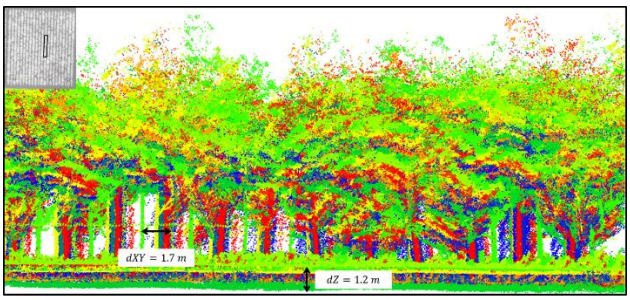

Figure 6. Side view of a profile from the *BP-2021* dataset (colored by time) generated from the original trajectory for qualitative evaluation of the level of misalignment.

3. SYSTEM CALIBRATION AND TRAJECTORY ENHANCEMENT STRATEGY

This section describes the proposed system-driven approach for system calibration and trajectory enhancement that can mitigate misalignments within the point cloud caused by inaccurate LiDAR mounting parameters and/or GNSS signal outages. The strategy is based on the hypothesis that any inaccuracy related to mounting parameters and platform trajectory would manifest in point clouds as misalignment among conjugate features, as shown earlier in Figure 4 and Figure 6. The framework of the proposed approach is summarized in Figure 7, which mainly comprises two parts. Part 1 focuses on extracting and matching planar and cylindrical features, whereas Part 2 covers the optimization framework for system calibration and trajectory enhancement. A brief description of each of the processing steps is presented below.

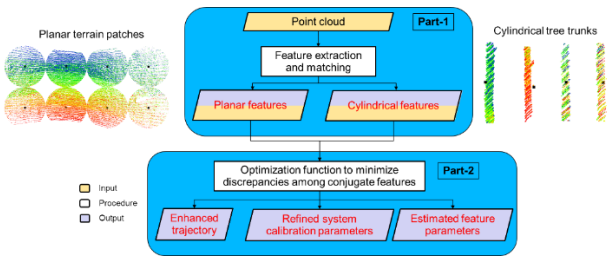

Figure 7. Proposed framework for system calibration and trajectory enhancement utilizing terrain patches and tree trunks.

3.1 Feature Extraction and Matching

It is assumed that UAV trajectories are of good quality given the platform's continuous access to GNSS signals. This assumption allows for using a combined point cloud from all tracks for reliable feature extraction. On the other hand, in the case of Backpack dataset, the assumption of a reasonably accurate point cloud for feature extraction is confined only to individual tracks. Based on these assumptions, point clouds either from the entire UAV dataset or from individual Backpack tracks are

reconstructed using the original GNSS/INS trajectory and LiDAR mounting parameters. Thereafter, a ground filtering algorithm based on adaptive cloth simulation approach (Lin et al., 2021b) is applied to generate a digital terrain model (DTM) and separate bare-earth (BE) points from above-ground (AG) ones based on certain height threshold (e.g., 0.5 m). The AG and BE points are respectively used for conducting extraction/matching of individual tree trunks and terrain patches.

Terrain patch extraction and matching for vertical control:
With the assumption that ground within a local neighbourhood can be approximated as a plane, terrain patches, which are extracted from BE points and matched among individual tracks and/or different datasets, are used as planar features to provide vertical control for system calibration and trajectory enhancement. The process starts by generating regularly spaced 2D seed points over the ROI where the Z coordinates are derived from the DTM. Through a local neighbourhood search and iterative plane-fitting, segmented points and parameters defining respective plane models are derived. Figure 8 visualizes sample terrain patches extracted from one track of the BP-2021 dataset. Once terrain patches from different point clouds are extracted, features are matched if they are extracted from the same seed point and if the angle between their normal vector is smaller than a user-defined threshold.

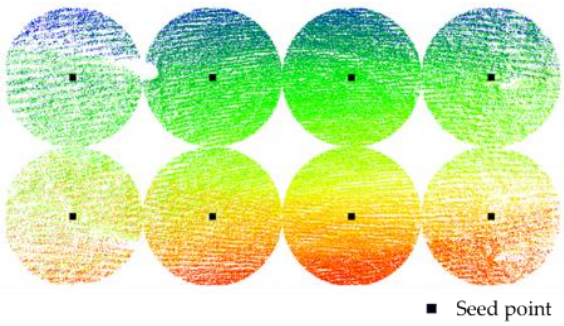

Figure 8. Sample planar features (terrain patches) extracted from the point cloud (colored by time).

Tree trunk extraction and matching for horizontal control:
Tree trunks are defined as cylindrical features to provide horizontal control. For tree trunk extraction, a lower portion of the AG points are isolated based on user-defined minimum and maximum height thresholds of h_{min} and h_{max} (e.g., 1.5 m and 3.5 m) above the DTM, as shown in Figure 9. Thereafter, a tree detection and localization approach is used to identify individual tree trunk in the hypothesized trunk portion (Lin et al., 2021a). Once the planimetric locations of individual tree trunks are known, seed points corresponding to the trunk portion are defined at a user-specified height ΔZ above the DTM, where ΔZ is chosen somewhere between the minimum and maximum height thresholds. Through a dimensionality-based analysis (Demantké et al., 2012) and an iterative model-fitting, a cylinder feature is identified. Finally, a region-growing is performed to augment neighbouring points that belong to the current feature evaluated based on whether their normal distances from the fitted cylinder are smaller than a factor of the root-mean-square (RMS) of fitting error. Figure 9 shows sample tree trunks extracted from an individual track of the *BP-2021* dataset. Once tree trunks from all point clouds have been extracted, conjugate features are matched if the planimetric distance between two seed points is less than a distance threshold (e.g., 1 m) and the angle between cylinders' axes is smaller than an angle threshold (e.g., 10°).

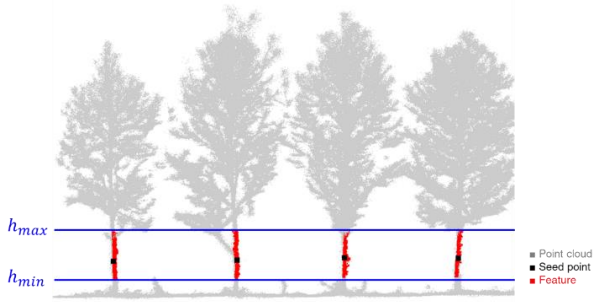

Figure 9. Minimum and maximum height thresholds used for tree trunk extraction and sample cylindrical features (tree trunks in red) extracted from the point cloud.

3.2 Optimization Framework for System Calibration and Trajectory Enhancement

The planar/cylindrical features extracted and matched from single or multiple datasets are used to refine system calibration parameters and enhance the quality of GNSS/INS trajectory. Conceptually, the proposed optimization framework aims at minimizing the normal distance between LiDAR points and the respective parametric models for planar/cylindrical features through a non-linear LSA. The basis of this optimization is the point positioning equation. Accordingly, for any LiDAR point I captured at time t, its coordinates in the mapping frame, $r_I^m(t)$, is a function of the coordinates of the point in laser unit frame, $r_I^{lu(t)}$, derived from raw measurements at their firing time, trajectory position and orientation parameters at the corresponding time $\left(r_{b(t)}^m, R_{b(t)}^m\right)$, and LiDAR mounting parameters which includes lever arm and boresight angles $\left(r_{lu}^b, R_{lu}^b\right)$. The mathematical model is symbolically expressed by Equation (1). Subsequently, the corrected coordinates of the same LiDAR point after system calibration and trajectory enhancement will depend on the refined mounting parameters $\left(r_{lu}^b(\text{refined}), R_{lu}^b(\text{refined})\right)$, and estimated corrections to the trajectory position/orientation parameters $\left(\delta r_{b(t)}^m, \delta R_{b(t)}^m\right)$, as expressed in Equation (2).

$$r_I^m(t) = f\left(r_{b(t)}^m, R_{b(t)}^m, r_{lu}^b, R_{lu}^b, r_I^{lu(t)}\right) \quad (1)$$

$$r_I^m(t)_{\text{corrected}} = f\begin{pmatrix} r_{b(t)}^m, \delta r_{b(t)}^m, R_{b(t)}^m, \delta R_{b(t)}^m, \\ r_{lu}^b(\text{refined}), R_{lu}^b(\text{refined}), r_I^{lu(t)} \end{pmatrix} \quad (2)$$

It is worth noting that solving the trajectory corrections at every timestamp of the observations is impractical as that would lead to over-parametrization in the LSA. Since the platform dynamics are moderate, the original high frequency trajectory (typically 100-200 Hz) is down-sampled to a user-defined rate, where the down-sampled trajectory points are denoted as trajectory reference points. The corrections to the trajectory parameters at a specific laser beam firing timestamp are then modelled as p^{th}-order polynomial functions of estimated corrections for their n neighboring trajectory reference points.

The mathematical model of the proposed LSA comprises two sets of constraints. The first set of constraints aims at minimizing the normal distance of each LiDAR point from the parametric model of its corresponding planar/cylindrical feature. The second set of constraint equations is introduced to minimize the change in position and orientation parameters for each trajectory reference point as well as the change in the distance traversed between two consecutive trajectory reference points depending on the standard

deviation reported by the GNSS/INS post-processing. It is worth mentioning that due to the potential correlation between the LiDAR mounting parameters and trajectory corrections, conducting a simultaneous optimization could lead to inaccurate estimation of the involved parameters. Thus, at a time, only one set of parameters is estimated while fixing the other. Ultimately, the LSA for system calibration and trajectory enhancement is conducted iteratively until the change in the RMS normal distance from LiDAR points to corresponding features becomes less than a pre-defined threshold.

4. EXPERIMENTAL RESULTS

This section presents experimental results to evaluate the performance of the proposed system calibration and trajectory enhancement strategy in terms of the improvement in the alignment of UAV and Backpack MMS points clouds. For all three datasets, the radius of terrain patches was set to 1 m. On the other hand, the minimum/maximum height thresholds for tree trunks were set to 0.5 m/2.5 m for *UAV-2021*/*BP-2021* datasets and 1.5 m/3.5 m for *UAV-2022* dataset. The reason behind this difference was the existing debris from tree thinning activity in the *UAV-2022* dataset. Table 2 lists the count of extracted features from each of the three datasets. The fewer tree trunks in the UAV-2022 dataset are due to the thinning activity as mentioned above. For the Backpack dataset, the large misalignments in the point cloud required manual quality control to ensure the accuracy of tree trunk matching. Since a part of this study aims at investigating the impact of integrating UAV and Backpack point clouds, features from the *BP-2021* and *UAV-2021* datasets were matched, resulting in 3,041 and 817 terrain patches and tree trunks, respectively.

Dataset	Cylindrical feature (Tree trunks)	Planar feature (Terrain patches)
UAV-2021	843	3,248
UAV-2022	540	
BP-2021	929	

Table 2. Number of the planar/cylindrical features extracted from the three datasets.

For conducting trajectory enhancement, the trajectory reference points were established at a frequency of 1 Hz (down-sampled from 200 Hz and 100 Hz for UAV and Backpack systems, respectively). Finally, the performance of the proposed approach was evaluated based on:

a) Estimated trajectory corrections: This is reported using statistical measures (mean, STD, RMS, and magnitude) of the corrections.
b) Relative accuracy of derived point clouds: The relative accuracy is qualitatively assessed by checking the alignment of point clouds. Quantitative assessment includes statistical measures of normal distances between LiDAR point and corresponding best-fitting plane/cylinder model before and after trajectory refinement.
c) Absolute accuracy of derived point clouds: Results from UAV datasets are used as a reference to analyse the absolute accuracy of Backpack point clouds after trajectory refinement.

4.1 System Calibration and Trajectory Enhancement for UAV Datasets

In this study, system calibration and trajectory enhancement were conducted sequentially on each UAV dataset to avoid any potential correlations among their parameters. At first, corrections to trajectory reference points were set to zero and fixed while estimating the system calibration parameters in the LSA. The Z lever arm component was also fixed in this process, as estimating it requires additional vertical control, which is not available for these datasets (Ravi et al., 2018b). The initial and refined system calibration parameters, along with their STD values, are presented in Table 3, where one can notice that the STD values are small. Subsequently, in the second LSA, the refined mounting parameters are fixed and then the trajectory corrections are estimated. Figure 10 shows the improvement in point cloud quality after each LSA process, where the initial point cloud of a sample tree (in red) is slightly improved after using the refined mounting parameter (in blue). However, the misalignment still exists, and only after the trajectory enhancement, the alignment is seen to improve significantly in both X and Y directions. The improvement in trajectory is statistically measured based on the RMS of differences between initial and refined position and orientation parameters for the UAV datasets. Accordingly, the RMS values for position parameters are in the range of 2 – 4 cm. Among the orientation parameters, RMS values for $\Delta\omega$ and $\Delta\phi$ are in the range of $0.03°$ – $0.06°$. On the other hand, the heading angle, $\Delta\kappa$, has a larger RMS value of around $0.15°$. This large heading correction, whose impact is along the flying direction (X coordinate), explains the worse alignment along the X direction before trajectory enhancement, as observed earlier in Figure 10.

For a quantitative evaluation of the performance of the proposed system calibration and trajectory enhancement, Table 4 reports the mean, STD, and RMS values of normal distances between the LiDAR feature points and their corresponding best-fitting plane/cylinder before and after the two-step LSA. Based on the RMS of normal distances, one can notice major improvements in the alignment of tree trunks after the two-step LSA for both UAV datasets. The smaller RMS value associated with cylindrical features for the *UAV-2021* dataset compared to that for *UAV-2022* is due to the larger height range used for the extraction of tree trunk features in the latter to avoid the inclusion of woody debris. This resulted in the extraction of tree branches mistakenly which increased the point-to-cylindrical feature normal distance.

	Mounting Parameters	$\Delta\omega(°)$	$\Delta\phi(°)$	$\Delta\kappa(°)$	$\Delta X(m)$	$\Delta Y(m)$	$\Delta Z(m)$
UAV-2021	Initial	0.499	-0.132	-0.092	-0.140	0.036	0.000
	Refined	0.466 ±0.001	-0.249 ±0.002	-0.193 ±0.003	-0.133 ±0.001	0.042 ±0.001	N\A
UAV-2022	Initial	1.261	-0.276	0.129	-0.115	0.022	0.100
	Refined	1.202 ±0.001	-0.295 ±0.002	-0.139 ±0.003	-0.095 ±0.001	0.010 ±0.001	N\A

Table 3. Initial and refined mounting parameters using the proposed system calibration approach for the *UAV-2021* and *UAV-2022* datasets.

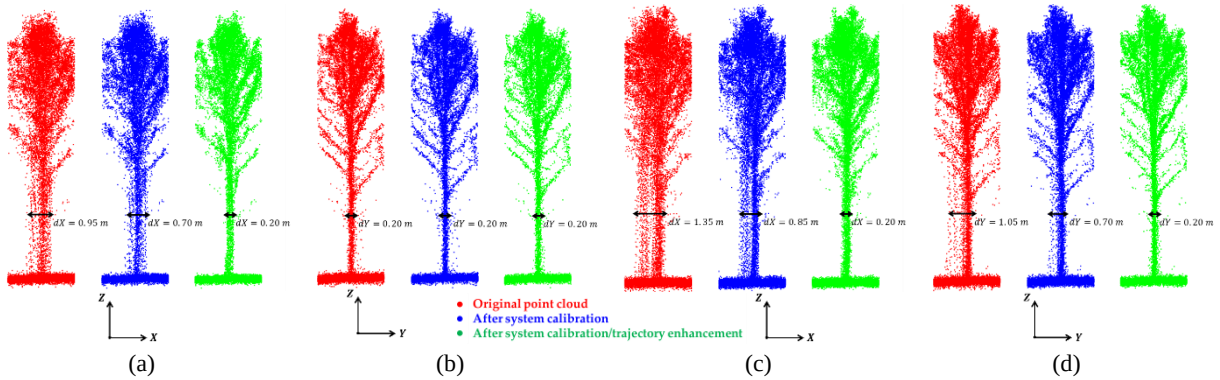

Figure 10. A sample tree in the original point clouds (in red), point clouds after system calibration (in blue), as well as point clouds after conducting system calibration and trajectory enhancement (in green): *UAV-2021* dataset views along (a) X-Z and (b) Y-Z planes, as well as *UAV-2022* dataset views along (c) X-Z and (d) Y-Z planes.

Dataset	Point-to-feature Normal Distance	# points (thousands)	Before LSA			After LSA		
			Mean (m)	STD (m)	RMS (m)	Mean (m)	STD (m)	RMS (m)
UAV-2021	Planar Features	10,313	0.036	0.037	0.052	0.032	0.033	0.046
	Cylindrical Features	412	0.107	0.106	0.151	0.048	0.053	0.072
UAV-2022	Planar Features	10,698	0.056	0.054	0.078	0.038	0.041	0.056
	Cylindrical Features	310	0.181	0.147	0.233	0.061	0.076	0.097

Table 4. Quantitative evaluation of point cloud alignment before and after sequential system calibration and trajectory enhancement for the UAV datasets.

Whereas the above evaluation was focused on the relative accuracy of each UAV dataset, the absolute accuracy of the point clouds after the proposed system calibration and trajectory enhancement is validated by analysing the alignment of point clouds from different UAV datasets. For the qualitative evaluation of the point cloud, Figure 11 shows a sample tree from the two UAV datasets after their sequential system calibration and trajectory enhancement. From the figure, it can be clearly seen that the tree trunks and branches are well-aligned in both X and Y directions. The slight misalignment in the Z direction is mainly because of the Z lever arm components of the two UAV systems that were derived through manual measurement and fixed in the LSA. Table 5 presents the quantitative evaluation of the point cloud alignment based on the extracted features. The mean, STD, and RMS values of the X and Y coordinate differences as well as the planimetric distances between tree locations indicate that the tree locations are in agreement with an accuracy of 0.1 m. The shift in the vertical direction is consistent with the Z discrepancy observed in Figure 11. Based on the results, hereafter, the *UAV-2021* dataset is used to evaluate the absolute accuracy of the Backpack point cloud, which will be discussed in the subsequent section.

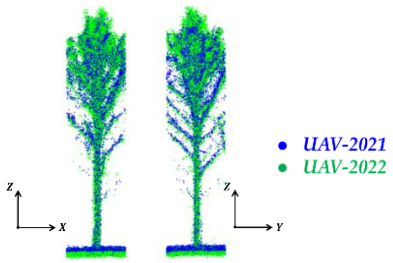

Figure 11. A sample tree from the point clouds after sequential system calibration and trajectory enhancement for the *UAV-2021* (in blue) and *UAV-2022* (in green) datasets along the X-Z and Y-Z planes.

4.2 Trajectory Enhancement Results for Backpack Dataset

For the *BP-2021* dataset, two tests were conducted to evaluate the performance of the proposed trajectory enhancement approach:

- Test 1: Trajectory enhancement using original trajectory with frequent access to open sky at the beginning and end of each track, and
- Test 2: Trajectory enhancement using lower-quality trajectory aided by the *UAV-2021* dataset. To be specific, LiDAR features from both the Backpack and UAV datasets were simultaneously included in the LSA. For the *UAV-2021* dataset, its refined mounting parameters and enhanced trajectory were treated as errorless.

First, the relative accuracy of the Backpack point clouds from the two tests is evaluated. Figure 12 shows a profile from the *BP-2021* dataset after trajectory enhancement for the two conducted tests. One can notice a significant improvement in tree trunk alignment when compared to the point clouds derived using the original trajectory (as shown in Figure 6). Results from Test 2, where the Backpack dataset is aided by the UAV dataset, show that even with the low-quality trajectory, the resulting point cloud can reach the same quality as in Test 1. The RMS of differences between initial and refined position parameters for Tests 1 and 2 have respective ranges of 0.19 – 0.26 m and 0.26 – 1.1 m, which indicates that Test 2 needed relatively severe corrections. Among the orientation parameters, RMS values for $\Delta\omega$ and $\Delta\phi$ are in the range of 0.005° – 0.03° and 0.03° – 0.07° for respective tests. For $\Delta\kappa$, i.e., the heading parameter, RMS values are 0.12° and 0.35°, respectively for Tests 1 and 2, which suggests higher corrections in the case of latter. For further quantitative evaluation, Table 6 reports the mean, STD, and RMS values of normal distance of the LiDAR points to their corresponding best-fitting plane/cylinder before and after the LSA process for the two tests. The RMS values after trajectory enhancement for both

Tests 1 and 2 are under 4 cm and 3 cm for planar and cylindrical features, respectively. This means that with the help of UAV point clouds, the adjustment process achieved an overall high relative accuracy using the low-quality Backpack trajectory.

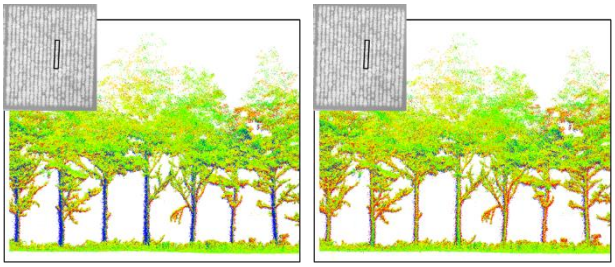

(a) (b)

Figure 12. Side view of a profile from the *BP-2021* dataset (coloured by time) after trajectory enhancement depicting the alignment quality for (a) Test 1 and (b) Test 2.

The absolute accuracy of the Backpack point cloud after trajectory enhancement is evaluated through a comparison with the refined point cloud from the *UAV-2021* dataset. Figure 13 shows a sample tree after Tests 1 and 2 on the Backpack dataset overlaid with the refined UAV point cloud. From the figure, one can see that the tree trunks from all three datasets are in good agreement in both X and Y directions. For the vertical direction, Test 2 shows slightly better alignment with the *UAV-2021* point cloud. Table 7 reports the Z differences between the terrain patches as well as X/Y differences and planimetric distances between estimated tree locations from the *BP-2021* and *UAV-2021* datasets. With the inclusion of UAV point cloud, Test 2 achieved a better vertical accuracy than Test 1. The comparison of tree trunks reveals that the tree locations are in agreement with an accuracy of 0.1 m for both tests.

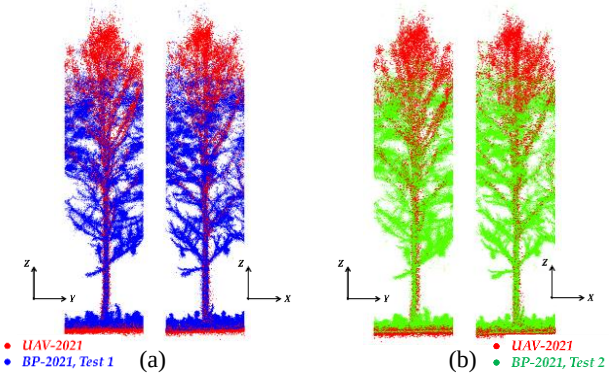

Figure 13. A sample tree in the Backpack point clouds after trajectory enhancement overlaid with the refined point cloud in the *UAV-2021* dataset (in red) along the X-Z and Y-Z planes: (a) Test 1 and (b) Test 2.

Comparison	Statistics Measures	Terrain Patches (3,248 features)	Tree Trunks (494 features)		
		dZ(m)	dX(m)	dY(m)	Planimetric Distance (m)
UAV-2021 vs. UAV-2022	Mean	-0.099	0.019	-0.059	0.097
	STD	0.037	0.055	0.089	0.073
	RMS	0.106	0.058	0.107	0.121

Table 5. Quantitative evaluation of the point cloud alignment between the *UAV-2021* and *UAV-2022* datasets after sequential system calibration and trajectory enhancement using terrain patches (for vertical direction) and tree trunks (for planimetric direction).

Tests	Point-to-feature Normal Distance	# points (thousands)	Before LSA			After LSA		
			Mean (m)	STD (m)	RMS (m)	Mean (m)	STD (m)	RMS (m)
Test 1	Planar Features	16,789	0.224	0.171	0.282	0.026	0.021	0.034
	Cylindrical Features	10,805	0.190	0.181	0.262	0.016	0.017	0.024
Test 2	Planar Features	16,789	0.713	0.941	1.180	0.027	0.023	0.036
	Cylindrical Features	10,805	0.355	0.246	0.432	0.021	0.021	0.029

Table 6. Quantitative evaluation of point cloud alignment before and after trajectory enhancement for the BP-2021 dataset.

Comparison	Statistics Measures	Terrain Patches (3,026 features)	Tree Trunks (788 features)		
		dZ (m)	dX (m)	dY (m)	Planimetric Distance (m)
BP-2021 Test 1 vs. UAV-2021	Mean	0.004	-0.005	-0.028	0.078
	STD	0.033	0.061	0.070	0.059
	RMS	0.034	0.062	0.075	0.097
BP-2021 Test 2 vs. UAV-2021	Mean	0.000	-0.029	-0.043	0.086
	STD	0.008	0.043	0.079	0.058
	RMS	0.008	0.052	0.090	0.104

Table 7. Quantitative evaluation of the absolute accuracy of the point cloud from the *BP-2021* dataset after trajectory enhancement through a comparison with the *UAV-2021* dataset using extracted terrain patches (for vertical direction) and tree trunks (for planimetric direction)

5. CONCLUSIONS AND RECOMMENDATIONS FOR FUTURE WORK

In this paper, a system-driven framework for system calibration and trajectory enhancement for LiDAR units mounted on UAV and Backpack MMS is proposed to generate accurate point clouds for high-resolution forest inventory. By minimizing the discrepancies among features from different tracks/datasets/systems while considering the absolute and relative positional/rotational information from the initial trajectory, system calibration parameters and trajectory information are refined through a non-linear LSA. The performance of the proposed strategy was evaluated using two UAV and one Backpack datasets. The results for the UAV datasets (after system calibration and trajectory enhancement) show a reduction in fitting error for the used terrain patches and tree trunks from 20 cm to 5 cm, and for the Backpack dataset (after trajectory enhancement), the fitting error reduced from 30 cm to 3 cm. For both the UAV and Backpack systems, the results suggest that the proposed trajectory enhancement approach enhanced the absolute accuracy to the 10 cm level.

The proposed and validated system calibration and trajectory enhancement framework for forest plantations will be used as the foundation for future research targeting accurate under-canopy mapping in rapidly changing natural forest environments. Further, modifications to the proposed algorithm will be investigated to increase its robustness to false tree trunk matching in cases where high misalignment within the point cloud might lead to a version of any tree trunk being matched with one of its neighbouring trees. Integrating raw IMU measurements, GNSS observations, and RGB imagery with LiDAR will be also explored to provide additional constraints to achieve trajectory with higher accuracy.

6. ACKNOWLEDGMENT

This work is supported in part by the U.S. Department of the Navy, Cooperative Ecosystem Studies Unit program (Agreement # N400852220004) and the U.S. Department of Agriculture, National Institute of Food and Agriculture, Sustainable Agriculture Systems project (2023-68012-38992).

REFERENCES

Barbeito, I., Dassot, M., Bayer, D., Collet, C., Drössler, L., Löf, M., del Rio, M., Ruiz-Peinado, R., Forrester, D.I., Bravo-Oviedo, A., Pretzsch, H., 2017. Terrestrial laser scanning reveals differences in crown structure of Fagus sylvatica in mixed vs. pure European forests. For Ecol Manage 405, 381–390. https://doi.org/10.1016/j.foreco.2017.09.043

Beland, M., Parker, G., Sparrow, B., Harding, D., Chasmer, L., Phinn, S., Antonarakis, A., Strahler, A., 2019. On promoting the use of LiDAR systems in forest ecosystem research. For Ecol Manage 450. https://doi.org/10.1016/j.foreco.2019.117484

Chiella, A.C.B., Machado, H.N., Teixeira, B.O.S., Pereira, G.A.S., 2019. GNSS/LiDAR-based navigation of an aerial robot in sparse forests. Sensors (Switzerland) 19. https://doi.org/10.3390/s19194061

Demantké, J., Mallet, C., David, N., Vallet, B., 2012. Dimensionality Based Scale Selection in 3D LiDAR Point Clouds. ISPRS Int. Archives of the Photogrammetry, Remote Sensing, and Spatial Information Sciences XXXVIII-5/, 97–102. https://doi.org/10.5194/isprsarchives-xxxviii-5-w12-97-2011

Goodbody, T.R.H., Coops, N.C., White, J.C., 2019. Digital Aerial Photogrammetry for Updating Area-Based Forest Inventories: A Review of Opportunities, Challenges, and Future Directions. Current Forestry Reports 55–75. https://doi.org/10.1007/s40725-019-00087-2

Habib, A., Lay, J., Wong, C., 2006. Specifications for the Quality Assurance and Quality Control of LiDAR Systems. Base Mapping and Geomatic Services of British Columbia 2006 [WWW Document]. URL https://engineering.purdue.edu/CE/Academics/Groups/Geomatics/DPRG/files/LIDARErrorPropagation.zip

Kelly, M., Tommaso, S. Di, 2015. Mapping forests with LiDAR provides flexible, accurate data with many uses. Calif Agric (Berkeley) 69, 14–20. https://doi.org/10.3733/ca.v069n01p14

Khosravipour, A., Skidmore, A.K., Isenburg, M., Wang, T., Hussin, Y.A., 2014. Generating pit-free canopy height models from airborne LiDAR. Photogramm Eng Remote Sensing 80, 863–872. https://doi.org/10.14358/PERS.80.9.863

Kukko, A., Kaijaluoto, R., Kaartinen, H., Lehtola, V. V, Jaakkola, A., Hyyppä, J., 2017. Graph SLAM correction for single scanner MLS forest data under boreal forest canopy. ISPRS Journal of Photogrammetry and Remote Sensing 132, 199–209. https://doi.org/10.1016/j.isprsjprs.2017.09.006

Lin, Y.C., Liu, J., Fei, S., Habib, A., 2021a. Leaf-off and leaf-on uav lidar surveys for single-tree inventory in forest plantations. Drones 5. https://doi.org/10.3390/DRONES5040115

Lin, Y.C., Manish, R., Bullock, D., Habib, A., 2021b. Comparative analysis of different mobile LiDAR mapping systems for ditch line characterization. Remote Sens (Basel) 13. https://doi.org/10.3390/rs13132485

Qian, C., Liu, H., Tang, J., Chen, Y., Kaartinen, H., Kukko, A., Zhu, L., Liang, X., Chen, L., Hyyppä, J., 2017. An integrated GNSS/INS/LiDAR-SLAM positioning method for highly accurate forest stem mapping. Remote Sens (Basel) 9. https://doi.org/10.3390/rs9010003

Ravi, R., Lin, Y.-J., Elbahnasawy, M., Shamseldin, T., Habib, A., 2018a. Simultaneous System Calibration of a Multi-LiDAR Multicamera Mobile Mapping Platform. IEEE J Sel Top Appl Earth Obs Remote Sens 11, 1694–1714. https://doi.org/10.1109/JSTARS.2018.2812796

Ravi, R., Lin, Y.J., Elbahnasawy, M., Shamseldin, T., Habib, A., 2018b. Bias impact analysis and calibration of terrestrial mobile LiDAR system with several spinning multibeam laser scanners. IEEE Transactions on Geoscience and Remote Sensing. https://doi.org/10.1109/TGRS.2018.2812782

Su, Y., Guo, Q., Jin, S., Guan, H., Sun, X., Ma, Q., Hu, T., Wang, R., Li, Y., 2020. The Development and Evaluation of a Backpack LiDAR System for Accurate and Efficient Forest Inventory. IEEE Geoscience and Remote Sensing Letters 18. https://doi.org/10.1109/lgrs.2020.3005166

White, J.C., Coops, N.C., Wulder, M.A., Vastaranta, M., Hilker, T., Tompalski, P., 2016. Remote Sensing Technologies for Enhancing Forest Inventories: A Review. Canadian Journal of Remote Sensing 42, 619–641. https://doi.org/10.1080/07038992.2016.1207484